Published online 31 December 2015 *Nucleic Acids Research, 2016, Vol. 44, No. 3* ***1271–1284***
doi: 10.1093/nar/gkv1474

Shade avoidance 6 encodes an *Arabidopsis* flap endonuclease required for maintenance of genome integrity and development

Yijuan Zhang[1,2], Chunhong Wen[1], Songbai Liu[3,4,5], Li Zheng[3], Binghui Shen[3] and Yi Tao[1,2,*]

[1]School of Life Sciences, Xiamen Plant Genetics Key Laboratory, Xiamen University, Xiamen 361102, China, [2]State Key Laboratory of Cellular Stress Biology, Xiamen University, Xiamen 361102, China, [3]Department of Cancer Genetics and Epigenetics, Beckman Research Institute of City of Hope, Duarte, CA 91010, USA, [4]College of Life Sciences, Zhejiang University, Hangzhou, China and [5]Suzhou Health College, Suzhou Key Laboratory of Biotechnology for Laboratory Medicine, Suzhou, 215009, Jiangsu Province, China

Received August 03, 2015; Revised December 03, 2015; Accepted December 03, 2015

ABSTRACT

Flap endonuclease-1 (FEN1) belongs to the Rad2 family of structure-specific nucleases. It is required for several DNA metabolic pathways, including DNA replication and DNA damage repair. Here, we have identified a shade avoidance mutant, *sav6*, which reduces the mRNA splicing efficiency of *SAV6*. We have demonstrated that SAV6 is an FEN1 homologue that shows double-flap endonuclease and gap-dependent endonuclease activity, but lacks exonuclease activity. *sav6* mutants are hypersensitive to DNA damage induced by ultraviolet (UV)-C radiation and reagents that induce double-stranded DNA breaks, but exhibit normal responses to chemicals that block DNA replication. Signalling components that respond to DNA damage are constitutively activated in *sav6* mutants. These data indicate that SAV6 is required for DNA damage repair and the maintenance of genome integrity. Mutant *sav6* plants also show reduced root apical meristem (RAM) size and defective quiescent centre (QC) development. The expression of *SMR7*, a cell cycle regulatory gene, and *ERF115* and *PSK5*, regulators of QC division, is increased in *sav6* mutants. Their constitutive induction is likely due to the elevated DNA damage responses in *sav6* and may lead to defects in the development of the RAM and QC. Therefore, SAV6 assures proper root development through maintenance of genome integrity.

INTRODUCTION

Higher plants grow as a result of the division of stem cells located at root/shoot apical meristems and lateral meristems. Meristem cells show high mitotic activity, and their division provides the cells needed for the generation of various tissues and organs. Roots of *Arabidopsis* can be divided into three sections: the root apical meristematic zone (RAM), elongation zone and maturation zone (1). Most of the cells in the RAM are actively dividing. The size of the RAM depends on the balance between the rates of cell division and cell differentiation. At the apical end of the root meristem, the stem cells surround 4–8 mitotically inactive cells, called the quiescent centre (QC). Together, these cells form a stem cell niche. The QC cells rarely divide; instead they maintain the undifferentiated state of the surrounding stem cells by sending short-range signals to surrounding cells and thus creating a microenvironment that prevents the differentiation of the stem cells (2). The QC cells are therefore critical for the normal development of the RAM. However, how the development and maintenance of QC cells are regulated remains largely unknown.

Cells are also constantly exposed to stresses that can lead to DNA damage. Similar to animal stem cells, plant RAM cells are particularly intolerant to DNA damage. In response to DNA damage, the DNA damage repair machinery is typically induced to correct the resulting base modifications and other DNA lesions. Furthermore, cell cycle arrest and cell death are often induced. ATAXIA TELANGIECTASIA MUTATED (ATM) and ATAXIA TELANGIECTASIA AND RAD3-RELATED (ATR) are protein kinases that play key roles in the DNA damage responses that are induced by double-stranded DNA breaks (DSBs) and single-strand DNA breaks/replication stress, respectively. For cell cycle regulation, a well-characterized target of ATM and ATR in plants is the Wee1-LIKE PROTEIN KINASE, WEE1. Transcripts of *WEE1* are strongly up-regulated by replication-inhibiting drugs in an ATR-dependent manner, and by γ-irradiation and radiomimetic drugs in an ATM-dependent manner (3). Induction of *WEE1* expression arrests the cell cycle at the S phase (4).

*To whom correspondence should be addressed. Tel: +86 592 2180852; Fax: +86 592 2181015; Email: yitao@xmu.edu.cn

Recently, Yi *et al.* reported that three members of the SIAMESE/ SIAMESE-RELATED (SIM/SMR) class of cyclin-dependent kinase inhibitors (*SMR4, 5* and *7*) were also strongly induced in response to genotoxic reagents in an ATM-dependent manner (5). They demonstrated that these SMR proteins are involved in cell cycle regulation during endoreplication, an atypical cell cycle consisting of repeated rounds of chromosomal replication without cell division, and the response to DNA damage. Therefore, in response to replication stress and DNA damage-induced stress, multiple cell cycle regulatory pathways may be activated. The specific roles of each pathway are not known yet.

Cell death is one possible outcome in response to DNA damage; the organism selectively kills individual cells with damaged DNA in order to preserve genome integrity at the whole-organism level. Fulcher and Sablowski demonstrated that root stem cells and their early descendents, but not QC cells, were selectively killed by reagents that induce DSBs but not agents that induce DNA replication stress (6,7). Heyman *et al.* hypothesized that after removing the DSB-inducing drug, the QC-expressing domain (cells expressing the QC marker *WOX5$_{pro}$:GFP*) expanded through cell division and replenished the dead stem cells within 2–4 days (6) and this recovery process may require ETHYLENE-RESPONSIVE FACTOR 115 (ERF115), a transcriptional activator of *PSK5*, which is a precursor gene for the plant PEPTIDE GROWTH HORMONE PHYTOSULFOKINE-α (PSK-α). Over-expression of *ERF115* promoted QC cell division, which is dependent on PSKR1, a PSKα receptor (6). Therefore, QC cells are critical for the recovery from DNA damage-induced cell death and *ERF115* and *PSK5* are key genes that control QC cell division.

Human flap endonuclease1 (FEN1) is a member of the radiation-sensitive 2(RAD2) nuclease family. It recognizes specific structures of the substrates and possesses flap endonuclease (FEN), 5′ exonuclease (EXO) and gap endonuclease (GEN) activities. FEN1 is best known for its essential roles in the processing of Okazaki fragments during replication of the lagging strand and for long-patch base excision repair (BER), which requires FEN activity. It is also required for the resolution of tri-nucleotide repeat-derived secondary structures, rescue of stalled replication forks, maintenance of telomere stability and apoptotic DNA fragmentation (8–10). Null mutations in *Rad27*, a yeast FEN1 homologue, result in slow growth, hypersensitivity to DNA-damaging reagents and genome instability, and homozygous *Fen1* knock-out in mice is embryonic lethal (11–13). Two FEN1 homologues were identified in rice (*Oryza sativa, OsFEN1a, OsFEN1b*). Functional complementation tests revealed that only *OsFEN1a* can complement the yeast *fen1*/*rad27* mutant, suggesting that the two genes may be functionally distinct (14). Furthermore, OsFEN1a, expressed in *Escherichia coli,* possesses both FEN and EXO nuclease activity (15). In *Arabidopsis thaliana*, one FEN1 homologue was identified through a homology search, but no further characterization was reported (14). No phenotype associated with FEN1 mutation in plants has been described so far.

We identified a *shade avoidance 6* (*sav6*) mutant that is defective in root and hypocotyl elongation. The mutation in *sav6* reduced the mRNA splicing efficiency of *SAV6*, which encodes an *Arabidopsis* FEN1 (AtFEN1). Biochemical characterization of SAV6 revealed that, unlike the animal FEN1, SAV6 shows FEN and GEN activity, but lacks EXO activity. However, like the human FEN1 (hFEN1), SAV6 is also required for the maintenance of genome integrity and response to DNA damage in plants. *sav6* mutants exhibit reduced RAM size and defects in QC development. Our study revealed that elevated responses to DNA damage in *sav6* increase the expression of *SMR7* and activate the ERF115-PSK5 pathway, which inhibits cell cycle progression and induces QC division, respectively. This suggests that SAV6 ensures proper root development through the maintenance of genome integrity.

MATERIALS AND METHODS

Plant materials and growth conditions

Arabidopsis seeds were surface sterilized with ethanol. The seeds were then sown onto $\frac{1}{2}$ MS with 0.8% agar. After stratification for 3 days, the plates were placed in continuous white light (Wc, 100 μmol/m^2/s, 22°C) for 3 days. For the root assays, the seedlings were grown vertically. *QC46*:*GUS*, *QC25*:*GUS* (16) and *WOX5$_{pro}$*:*GFP* expresses β-glucuronidase (GUS) or GFP under control of the indicated promoters (17). Analysis using *SAV6$_{pro}$:SAV6g*/*sav6* were performed on two independent lines (L1 and L2). For the marker studies, only phenotypes observed in all three lines are reported.

RNA isolation and qRT-PCR analysis

Total RNA was extracted from root tips that were shorter than 5 mm using the TriPure (Roche) reagent. The RNA was used for reverse transcription (cDNA Synthesis Kit K1622; Thermo Scientific). qRT-PCR was carried out using SYBR green reagents and a Stratagene Mx3000p real-time PCR system (AGILENT Technologies). Unless otherwise specificied, the relative expression of each gene was calculated by first normalizing to the expression of a reference gene *REF3* (*At1g13320*, *PP2A*), using the ΔΔ Ct method (18) and then calculate the ratio between the relative expression of the gene to its expression in Col-0 or untreated control samples. The standard error was calculated from three replicates.

Histochemical assays and microscopy

GUS and PI staining were performed as previously described (19,20). The root tips were stained with lugol solution (Sigma-Aldrich). For the measurement of hypocotyl cell number and cell length, it was done as previous described (21). For cell length measurements, images of the rapidly-elongating hypocotyl cells (the 8th–12th cell in Col-0 and the 5th–9th in *sav6*, counting from the junction of the root and hypocotyl to the shoot apical meristem) were taken and then measured using Scion Image software (http://www.scioncorp.com).

Phylogenetic analysis

The unrooted phylogenetic tree was drawn based on the alignment with the MEGA software. A neighbour joining tree based on the conserved region is shown. Sequences used here are available in Supplementary Data 1.

Hypocotyl and root length measurement

The seedlings were first scanned and the hypocotyl and root lengths were measured on scanned images using Scion Image.

Drug response tests

For the responses to camptothecin (CPT, Merck) and hydroxyurea (HU, Sigma-Aldrich), 3-day-old seedlings were transferred to $\frac{1}{2}$ MS plates containing various drugs. Root length was then measured 5 days later. For the responses to Zeocin (Invitrogen), roots of 3-day-old seedlings were immersed in $\frac{1}{2}$ MS containing 60 μg/ml of Zeocin for 12 h, followed by PI staining. For the responses to UV-C, 6-day-old, light-grown seedlings were irradiated with UV-C. They were then allowed to recover in Wc for 6 days before chlorophyll measurement. For the root length measurements, the seedlings were grown vertically. Root growth after recovery was measured.

Transgenic plants

For the *SAV6$_{pro}$:SAV6g /sav6* transgenic lines, a DNA fragment containing the *At5g26680* 2842bp promoter sequence, *SAV6* genomic DNA (3577 bp) and 578bp *SAV6* 3′ UTR was amplified from Col-0 and cloned into *pJHA212K*. The *SAV6$_{pro}$:GUS*/Col-0 transgenic lines was generated by inserting *SAV6* promoter and 3′-UTR fragment into the *pJHA212K-GUS* vector (22). To generate the *35S:SMR7:3XFLAG*/Col-0 transgenic lines, the coding sequence of *SMR7* was amplified and inserted into the *pPZP212–3X FLAG* (23). To generate the *35S:amiR172a-SMR7/sav6* transgenic lines, the mature *miR172a* sequence from *pDONR201-miR172a* (a gift from Dr Huang, Tao) was exchanged with the highly specific 21 bp of *SMR7* (5′-ATCACTCCCACGGCGAGAGGA-3′) according to the manufacturer's instructions (KOD-Plus-Mutagenesis Kit; TOYOBO) to obtain *pDONR201-amiR172a-SMR7* (24). Then the *amiR172a-SMR7* fusion gene was subcloned into the *pK2GW7* destination vector using LR Clonase (Invitrogen Gateway® LR Clonase® II Enzyme mix). The primer sequences were provided in Supplementary Table S1.

FEN1 nuclease activity assays

The coding sequence of the full-length *SAV6* gene was fused to the *pMBP-C-GST-His* vector. hFEN1 and SAV6 were expressed and purified following published protocols (25,26). ^{32}P-labelled flap DNA substrates A, B, C, D and E were prepared, using the oligo-nucleotides listed in Supplementary Table S2, as described previously (27). The nuclease activity assays were also set up following an established protocol (28). Briefly, the indicated amount of FEN1 protein or SAV6 protein was incubated with substrates for 5, 10, 20, 40, 60 and 80 min. The amount of the enzyme used in various reactions is indicated in the figure legends. The reactions were carried out in a total volume of 10 μl at 37°C and analysed by denaturing 15% polyacrylamide gel electrophoresis (PAGE). The products were visualized by autoradiography and quantified using Image J.

Yeast assays

SX46A and Δrad27:TRP1 were gifts from Dr Michael S. Reagan (11). The survival assays and the sensitivity to DNA-damaging agents assays were done as previously described (11).

Map-Based cloning

sav6 was crossed to Ler-erecta to generate F2 mapping population. The Monsanto Arabidopsis Polymorphism and Ler Sequence Collections and Arabidopsis Mapping Platform were used to design mapping markers.

RESULTS

sav6 mutants have short hypocotyls and roots

sav6 was first identified as a shade avoidance mutant that was defective in shade-induced hypocotyl elongation in a forward genetic screen using EMS-mutagenized Col-0 (22). Phenotypic characterization was carried out after backcrossing *sav6* with Col-0 for three generations. Further characterization revealed that, compared to the Col-0 wild type, the hypocotyls of *sav6* were short in Wc, simulated shade and darkness (Figure 1A), suggesting that the hypocotyl elongation defect of *sav6* is light-independent. Furthermore, we observed that the primary roots of *sav6* mutants were much shorter than those of the wild type, especially during early seedling development (Figure 1B). However, we also noted that as the mutant seedling continues growing, a new root emerges, which replaces the primary root and becomes dominant (Supplementary Figure S1A). This new root is only slightly shorter than the primary root of the wild type after 8 days in Wc (Supplementary Figure S1B).

Map-based cloning of *sav6*

Through map-based cloning (29), we determined that the mutation is located on chromosome 5. Fine mapping results further narrowed down the site of the mutation to a region between 9.30 and 9.36 MB. Through direct sequencing, we identified a G-to-A transition at 9.314105 MB, which is the last nucleotide of the 9th exon of *At5g26680*. The mutation results in a synonymous substitution, which does not change the coded amino acid (Lys) (Supplementary Figure S2A). Because the mutation is located at the junction of the 9th exon and an intron, we wondered if the mutation would affect mRNA splicing. The primers were designed to span two exon-exon boundaries (RT-F/R) to avoid genomic DNA contamination (Figure 2A). We performed polymerase chain reaction (PCR) using cDNAs prepared from wild type and *sav6* seedlings. With wild type cDNAs, we expected to obtain a 555 bp fragment. If the

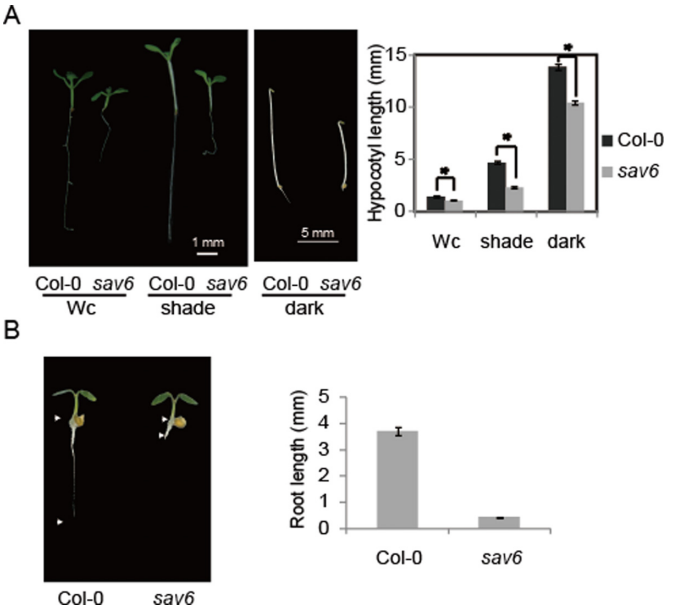

Figure 1. *sav6* has short hypocotyls and roots. (**A**) Hypocotyls of *sav6* seedlings grown in Wc, simulated shade, or darkness are shorter than those of the Col-0 wild type. Representative seedlings are shown in the left panel and quantitative measurements of hypocotyl length are shown in the right panel. *: *P*-value < 0.01, Student's t-test. (**B**) Roots of 3-day-old light-grown *sav6* seedlings are shorter than those of the wild type. Left panel: representative seedlings; right panel: quantitative measurements of root length. Error bars represent the standard error of the mean (SEM, $n \geq 14$).

9th intron (112 bp) was not spliced out, we would then obtain a 667 bp fragment. Indeed, through RT-PCR, we obtained one major band (about 555 bp) using wild type cDNAs, whereas an extra band (about 700 bp) was obtained using *sav6* cDNAs (Figure 2B). We cloned and sequenced both PCR products and confirmed that the small fragment has the wild type sequence and the larger fragment contains the 112 bp intron 9 sequence. Furthermore, the intensity of the wild type splicing product was significantly reduced in the *sav6* mutant compared to the wild type. The above result indicates that the mutation in *sav6* alters the mRNA splicing of the *At5g26680* gene and reduces its splicing efficiency. The translation of transcripts with an unspliced 9th intron would generate truncated proteins, as shown in the right panel of Figure 2B. *At5g26680* is annotated as a 5′-3′ exonuclease family protein (www.arabidopsis.org) or a flap endonuclease I (http://www.ncbi.nlm.nih.gov). The truncated protein contains the XPG (Xeroderma Pigmentosum Complementation Group G) N-terminal region but is missing the domain predicted to have XPG/RAD2 endonuclease activity. Therefore, the truncated form should not have any enzyme activity.

To verify the mapping result, we performed a complementation test. Genomic *SAV6* with its own promoter and 3′ UTR was cloned into the *pJHA212K* vector and transformed into the *sav6* mutant. The hypocotyl and root lengths of $SAV6_{pro}$*:SAV6g/sav6* transgenic seedlings were measured. As shown in Figure 2C, D and Supplementary Figure S1C, the short root and hypocotyl phenotypes of *sav6* were completely rescued by the transgene.

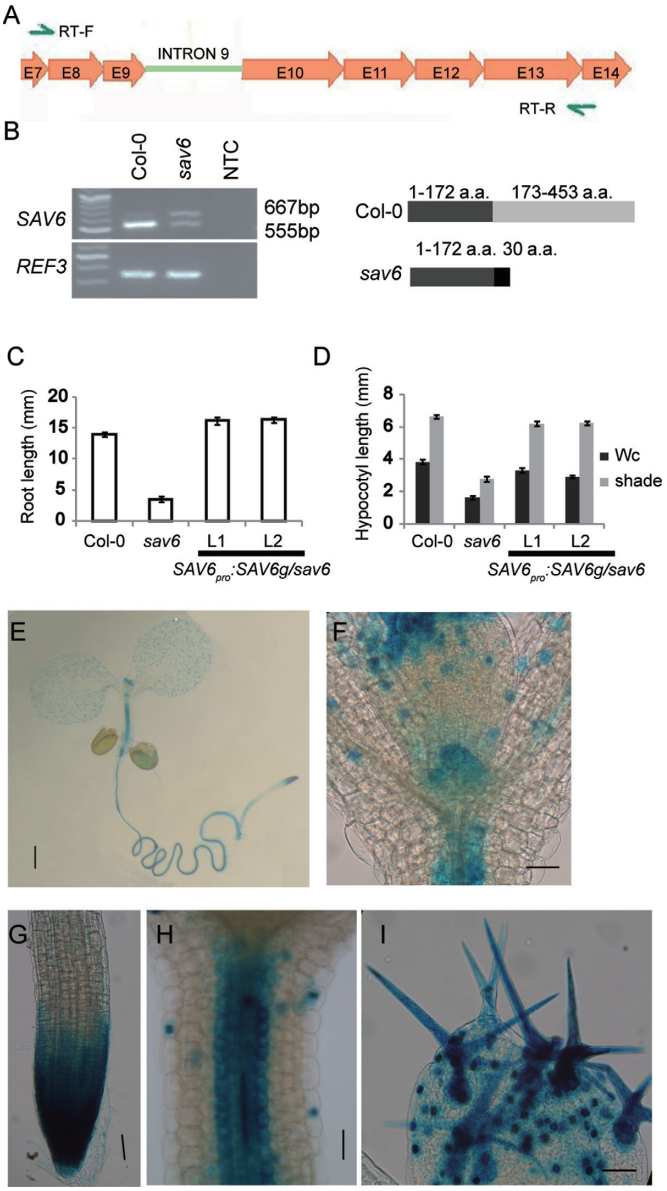

Figure 2. Cloning and characterization of *SAV6*. (**A**) Diagram showing the primers used to identify unspliced intron 9. E: exon; RT-F/R: PCR primers. (**B**) Inefficient splicing of intron 9 leads to reduced expression of functional *SAV6* in the mutants. Left panel: products of PCR reactions using cDNAs prepared from Col-0 and *sav6* as the templates and RT-F/R as the primers. Right panel: expected polypeptide sizes from the wild type and the mutant proteins. Failure to remove intron 9 would reveal a stop codon, leading to a truncated protein with 30 extra amino acids. (**C,D**) *SAV6* complements both the short root (C) and the short hypocotyl (D) phenotype of *sav6* mutants. Two independent transgenic lines ($SAV6_{pro}$*:SAV6g/sav6*, L1 and L2) were analysed. Error bars represent the SEM ($n \geq 15$). (**E–I**) *SAV6* expression analysis using $SAV6_{pro}$*:GUS* reporter line. More than three independent lines were analysed and expression patterns common in all three lines were shown. E: a 6-day-old light-grown seedling, F: emerging young leaves and shoot apical meristem; G: root tip; H: hypocotyl; I: trichomes. The scale bar in figure panel E represents 1 mm; for figure panels F-I, it represents 50 μm.

SAV6 expression pattern analysis

To analyse the organ- and tissue-specific expression pattern of *SAV6*, we generated transgenic lines expressing a *GUS* reporter gene under the control of the *SAV6* promoter (*SAV6$_{pro}$:GUS*). Histochemical localization of GUS activity revealed that *SAV6* was expressed in both roots and shoots (Figure 2E). Strong GUS activity was detected in proliferating cells including shoot and root apical meristems (Figure 2F and G), lateral root primordia (Supplementary Figure S2B), and developing carpels and stigmas (Supplementary Figure S2C). SAV6 was also highly expressed in the vascular tissue and the endodermal cells of the hypocotyls and roots (Figure 2H, Supplementary Figure S2B). In the leaves, GUS activity was detected in the guard cells and trichomes (Supplementary Figure S2D, Figure 2I). Expression of SAV6 was stronger in the progenitor cells of the stomatal lineage, such as the primary and satellite meristemoids, than in fully developed stomata cells (Supplementary Figure S2D). Trichomes are highly modified single cells that undergo several endoreplication cycles during their morphogenetic development (30–32). Endoreplication also occurs in hypocotyls after germination and in elongation/differentiation root cells. The expression pattern of SAV6 therefore suggests that SAV6 may function in both dividing cells and some of the cells that undergo endoreplication.

SAV6 encodes an *Arabidopsis* flap endonuclease I (AtFEN1)

BLAST analysis identified four potential SAV6 homologues, including UVH3, which is an *Arabidopsis* RAD2 (AtRAD2) or XPG-like protein, required for repair of pyrimidine-pyrimidone (6–4) dimers (33). We compared the protein sequences of these *Arabidopsis* proteins with FEN1 from different organisms. SAV6 exhibited the highest sequence similarity to rice FEN1s (OsFEN1a/b) (Figure 3A). OsFEN1a was demonstrated to possess FEN activity and was able to complement yeast *fen1* mutant, *Δrad27* (14,15).

Human FEN1 localizes to the nucleus during the S phase of the cell cycle or in response to DNA damage (34). To examine the subcellular localization of SAV6, we constructed transgenic plants expressing SAV6 tagged with a C-terminal YFP (*SAV6$_{pro}$:SAV6g:YFP*). The transgene rescued the *sav6* defects in roots (Supplementary Figure S3A), suggesting that the YFP-tagged SAV6 is functional. Using confocal microscopy, we detected strong constitutive YFP signals in the nucleus, which is consistent with functions of SAV6 in DNA metabolism. Furthermore, SAV6-YFP super-accumulates in small nuclear foci in some of the cells, suggesting a regulatory mechanism that is different from human FEN1 (Supplementary Figure S3B).

To test if SAV6 possesses FEN1-like functions, we transformed *SAV6* into the yeast radiation sensitivity 27 (*Rad27,* known also as *FEN1)* mutant *Δrad27*, which is a temperature-sensitive, conditional-lethal mutant. As shown in Figure 3B, *Δrad27* yeast grew normally at 30°C, but failed to grow at 37°C. SAV6-expressing *Δrad27* yeast grew normally under both conditions, similar to the wild type strains, indicating that SAV6 performs similar functions as Rad27. *Δrad27* is also hypersensitive to ultraviolet radiation (UV) and to genotoxic reagents such as EMS (11,35).

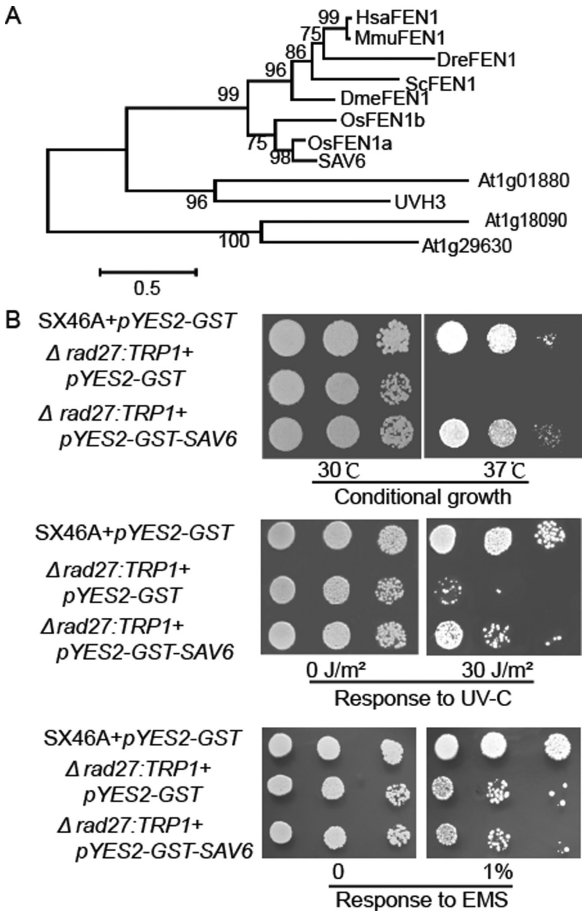

Figure 3. *SAV6* encodes an *AtFEN1*. (**A**) Phylogenetic analysis of SAV6/AtFEN1. Os: *Oryza sativa*, rice; Dre: *Danio rerio,* zebra fish; Hsa: *Homo sapiens,* human; Mmu, *Mus musculus,* mouse; Dme: *Drosophila melanogaster*, fly; Sc: *Saccharomyces cerevisiae,* yeast. Values below branches indicate bootstrap values. Bar = 0.5 amino acid substitutions per site. (**B**) SAV6 partially complements the yeast Rad27/FEN1 mutant rad27. Growth of a wild type (SX46A) yeast strain carrying an empty vector plasmid (*pYES2-GST*) or a rad27 mutant strain carrying either an empty vector or an *SAV6* cDNA with a glutathione S-transferase (GST) tag (*pYES2-GST-SAV6*) are shown. Growth of these strains on selection medium at the permissive (30°C) or restrictive (37°C) temperature (upper panel); with or without UV-C treatment (middle panel); and with or without ethyl methanesulfonate (EMS, lower panel) is shown.

SAV6 partially complemented the UV-C hypersensitivity of *Δrad27* (Figure 3B), but did not complement its EMS hypersensitivity (Figure 3B), suggesting that SAV6 may not have all the functions of Rad27. Alternatively, SAV6 may require other plant proteins for its full function.

We further characterized the nuclease activity profile of SAV6 using five standard substrates, based on a series of publications describing the hFEN1 substrates (10,36). These substrates include the following: a duplex double-flap DNA with a 3′ single-nt flap and a 40-nt-long 5′ flap, a substrate without the 3′ flap but with a 40-nt-long 5′ flap, one bubble structure duplex DNA, one nicked duplex DNA without any flap, and one gapped duplex DNA (with a 9-nt gap) without any flap. The substrates were incubated *in vitro* with purified hFEN1 or SAV6. As shown in Figure 4A–E, hFEN1 exhibited nuclease activity towards all five

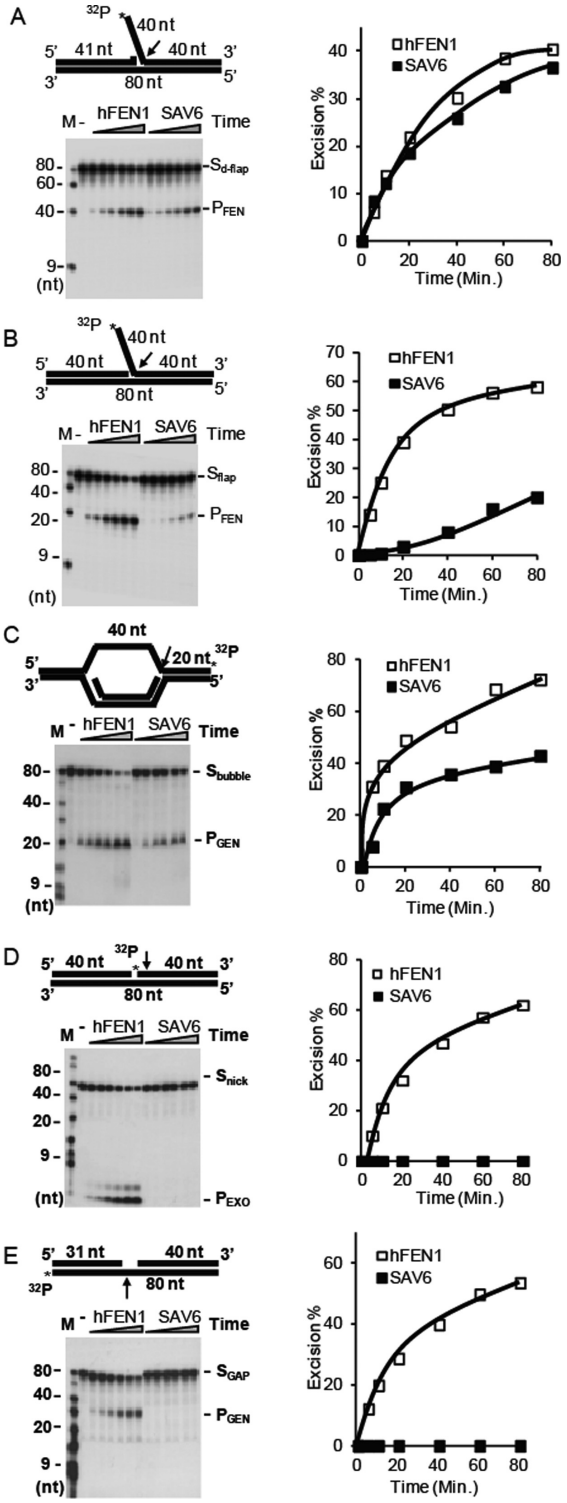

Figure 4. Nuclease activity profiles of hFEN1 and SAV6. (**A**) 33 nM hFEN1 or SAV6 was incubated with 3.3 nM ^{32}P labelled-double-flap DNA substrate ($S_{d\text{-}flap}$), which has a one-nucleotide 3′ flap and a 40-nt 5′ flap. (**B**) 33 nM hFEN1 or SAV6 was incubated with 33 nM of ^{32}P labelled-single-flap DNA substrate ($S_{s\text{-}flap}$), which has a 40-nt 5′ flap. (**C**) 66 nM hFEN1 or SAV6 was incubated with 33 nM ^{32}P-labeled bubble DNA substrate (S_{bubble}). (**D**) 66 nM hFEN1 or SAV6 was incubated with 33 nM ^{32}P-labeled nick DNA substrate (S_{nick}). (**E**) 66 nM hFEN1 or SAV6 was incubated with 33 nM gap substrate (S_{GAP}), in which the 3′ end of the template strand was labelled with ^{32}P.

substrates, demonstrating that hFEN1 can recognize all five types of substrates and exert its endonuclease/exonuclease activity. SAV6, on the other hand, had a different nuclease activity profile from that of the hFEN1. SAV6 effectively cleaved the duplex double-flap DNA at a similar efficiency to hFEN1 (Figure 4A). SAV6 also displayed activity on the single flap and bubble structure duplex DNA substrates, but its activity on these substrates was considerably weaker than that of hFEN1 (Figure 4B and C). Intriguingly, unlike hFEN1, SAV6 did not remove nucleotides from the 5′ end of the nicked duplex DNA substrate (Figure 4D) or cleave the template strand of the gapped duplex DNA substrate (Figure 4E). These data suggest that the substrate selection of SAV6 is more stringent than hFEN1.

Phenotypes of *sav6* resulting from altered cell division and differentiation

The short hypocotyls and roots of *sav6* mutants may result from a reduced cell number or reduced cell length, or both. We compared the hypocotyl epidermal cell profile of the Col-0 wild type and *sav6*. Wild type hypocotyls should consist of around 20 epidermal cells, and elongation of hypocotyls results mostly from cell expansion (reviewed by (37)). Our results showed that the epidermal cell number in *sav6* was reduced compared to that in the wild type, and this phenotype was rescued by the wild type *SAV6* gene (Figure 5A). We then measured the cell lengths of the hypocotyl epidermal cells, but found no significant differences in cell length between the Col-0 and *sav6* seedlings grown in Wc, simulated shade or darkness (Figure 5B). These results indicated that the short hypocotyls of *sav6* resulted from reduced cell number rather than reduced cell length, and the *sav6* mutation may affect hypocotyl cell division during embryogenesis.

Integrated cell proliferation and cell expansion controls the root length. As shown in Figure 5C, the size of the RAM is much smaller in *sav6* than in the wild type, which is indicated by both the length of the RAM and the number of cortex cells in the RAM. Cells in the elongation zone of the roots stop cell division and initiate differentiation. They undergo endoreplication and start to elongate. We measured the lengths of cells entering the maturation zone, where root hairs emerge. As shown in Figure 5D, these cells are over 150 μm in length in the wild type, whereas in *sav6*, they are only about 50 μm long. Both the reduced RAM size and the reduced cell length in the maturation zone were rescued by the wild type *SAV6* gene (Figure 5C and D). Therefore, SAV6 is required for both cell division and elongation in roots.

sav6 is defective in the maintenance of quiescent centre cells

During root development, QC cells function as stem cell organizing centres by creating a microenvironment that maintains the stem cell fate of its surrounding cells. In *sav6*, QC cells were difficult to identify (Figure 5C), so we crossed two widely used QC marker lines: *QC25:GUS* and *QC46:GUS* to *sav6*. As shown in Figure 5E, the blue GUS signals were detected specifically in QC cells in the wild type plants. In *sav6* mutants, however, signals from QC25 were dramatically reduced or completely absent, and those from

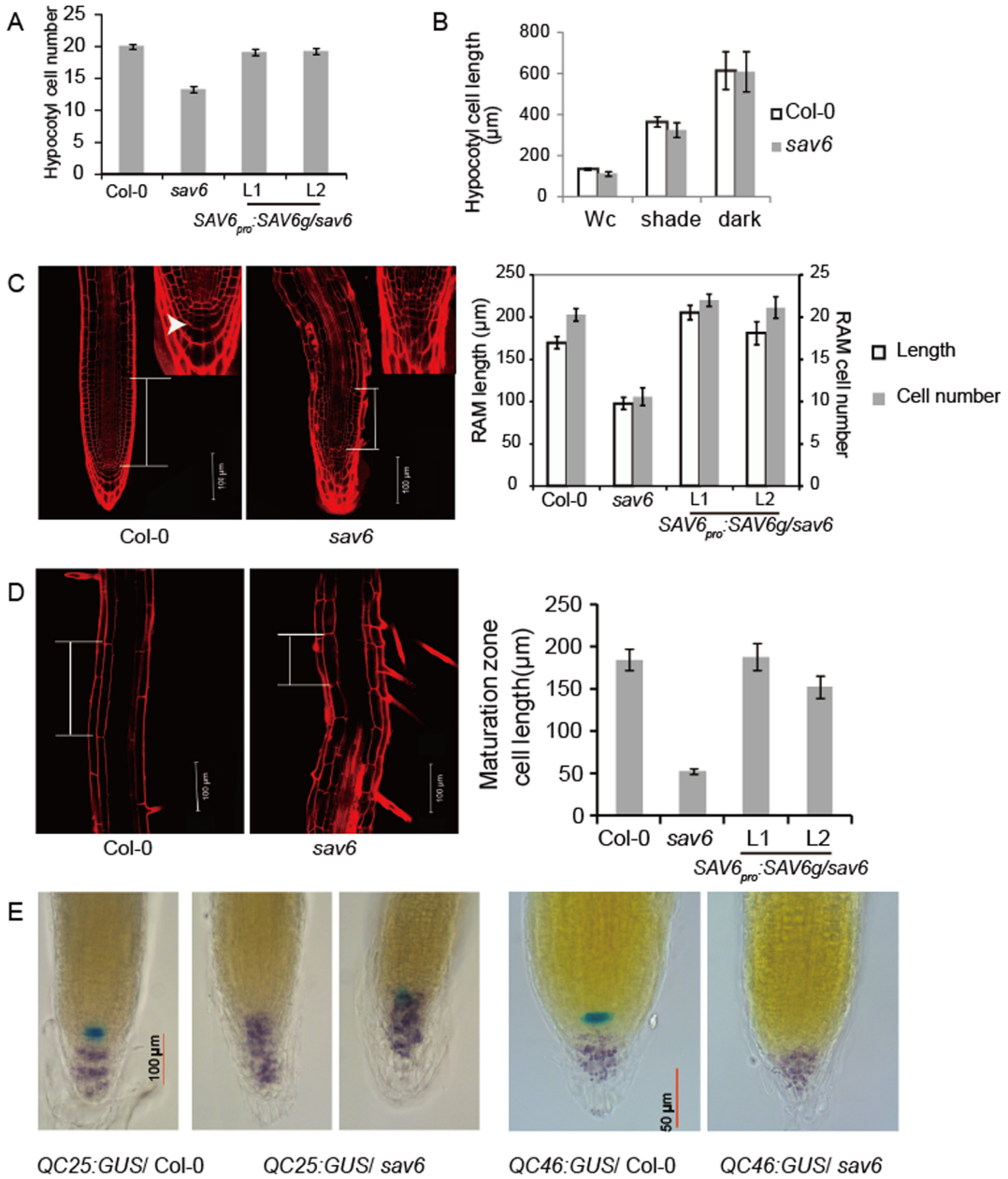

Figure 5. Mutation of *SAV6* affects both cell division and elongation. (**A**) Hypocotyl cell number is reduced in light-grown *sav6* relative to the Col-0 wild type ($n \geq 17$). (**B**) Hypocotyl cell length is not altered in seedlings grown in Wc, shade or darkness ($n \geq 8$). (**C**) Root apical meristem (RAM) size is reduced in *sav6*. Left panel: representative roots of Col-0 and *sav6*, with insets showing the root tips. The white arrowhead indicates the quiescent centre (QC) cells. The RAM zone lengths and the numbers of cortex cells are shown in the right panels ($n \geq 8$). (**D**) Cells in the maturation zone of *sav6* roots are shorter than those in the wild type. Left panel: representative roots; right panel: quantification of the cell length. Error bars represent the SEM ($n \geq 8$). (**E**) QC maintenance is compromised in *sav6* mutants. GUS staining shows that the expression of QC marker genes (*QC25 and QC46*) is reduced in *sav6*. Error bars represent the SEM.

QC46 were absent. Similar results were obtained when a $WOX5_{pro}$*:GFP* line was used (Supplementary Figure S4A). *WOX5* is a *WUSCHEL*-related *homeobox* gene that is expressed in QC cells and is required for the maintenance of stem cells. This QC defect was also largely rescued by the wild type *SAV6* gene (Supplementary Figure S4B). The above results indicate that the maintenance of QC cells is impaired in *sav6*.

SAV6 is required for recovery from UV-C induced DNA damage

Deletion of *yeast Fen1* (*rad27*) results in a high level of sensitivity to DNA damaging agents such as UV irradiation and methyl methane sulfonate, a strong mutator phenotype, and conditional lethality (11). It has been proposed that the coordinated action of the GEN and EXO activities of FEN1 are required for the survival of yeast cells in response to UV-C stress (27,38). We tested the response of *sav6* to UV-C.

The seedlings were treated with various doses of UV-C light and then allowed to recover for 5 days in light. As shown in Figure 6A, with increasing doses of UV-C irradiation, wild type seedlings became chlorotic and this response was much more dramatic in the *sav6* mutants. UV-C treatment also inhibited root elongation (Figure 6B), and this effect was again enhanced in *sav6*. These results indicate that SAV6 is required for the recovery from UV-C induced DNA lesions. Therefore, despite the lack of EXO activity, SAV6 is required for the survival of seedlings from UV-C-induced DNA damage, suggesting that the GEN activity of SAV6 may be critical for this damage recovery process.

SAV6 is required for the repair of DNA damage and the maintenance of genome integrity

FEN1 is required for both DNA replication and repair of damaged DNA. We tested the sensitivity of *sav6* to various genotoxic reagents. HU is a ribonucleotide reductase inhibitor that blocks DNA replication. *sav6* responded normally to HU, suggesting that the mutant can cope with replication stress normally (Supplementary Figure S5A). We then tested the responses of *sav6* to CPT and Zeocin, both of which induce DSBs. As shown in Figure 7A, the roots of *sav6* were hypersensitive to CPT-induced growth inhibition, and this effect was mostly rescued by expression of wild type *SAV6*. For Zeocin treatment, we used PI staining to detect dead cells in roots. As shown in Figure 7B, before Zeocin treatment, there were no dead cells detected in wild type seedlings, although 51% of *the sav6* roots exhibited mild staining. Zeocin treatment induced cell death in wild type seedlings and this effect was enhanced in *sav6* mutants. These effects of *sav6* were mostly suppressed by the introduction of *SAV6* genomic DNA (Supplementary Figure S5B). Therefore, the hypersensitivity of *sav6* mutants to reagents that induce DSBs suggested that SAV6 may be required for the repair of DSBs.

Because dead cells were detected in *sav6* mutants even without Zeocin treatment, we speculated that the responses to DNA damage were constitutively activated in *sav6* mutants. The expression levels of three DNA damage response genes: *RADIATION SENSITIVITY 51* (*RAD51*), *BREAST CANCER 1 EARLY ONSET* (*BRCA1*) and *POLY-ADP RIBOSE POLYMERASE 2* (*PARP2*) were examined (5) using quantitative real time PCR (qRT-PCR). Among them, RAD51 and BRCA1 are two DNA repair factors that are involved in the repair of double-strand DNA breaks, and the expression of *PARP2* is known to be induced by ionizing radiation and radiomimetic drugs (39,40). As shown in Figure 7C, the expression levels of all three genes were elevated in the roots of *sav6* mutants, which was also partially suppressed by the *SAV6* transgene (Supplementary Figure S5C), confirming that responses to DNA lesions are induced in *sav6* roots. It was previously reported that mild treatment with DSB-inducing reagents such as X-rays and radiomimetic drugs can induce cell death in stem cells and their early descendants, whereas, Aphidicolin, which specifically inhibits nuclear DNA replication, did not induce cell death (7). We therefore hypothesize that the DNA damage responses we observed in *sav6* may result from DSBs, but not DNA replication stress. Because HU can also induce the expression of the above three marker genes, we identified a marker gene, *At4g05370*, which is specifically induced by DSB-inducing gamma rays and bleomycin (5). As shown in Supplementary Figure S5D and S5E, both short term (1 and 3 h) and long term (12 and 24 h) Zeocin treatment elevated the expression of this gene. UV-C treatment also slightly increased its expression, but HU or Aphidicolin did not change its expression. In *sav6*, we also observed a significant increase in *At4g05370* expression, which was completely rescued by introduction of the genomic SAV6 transgene (Supplementary Figure S5F), supporting our hypothesis that the observed phenotypes and elevated expression of the marker genes in *sav6* may result from DNA damage stress, likely to be DSBs, but not from DNA replication stress.

Elevated expression of *SMR7* in *sav6* roots affects RAM development and helps to limit DNA damage-induced cell death

Both replication stress and response to DNA damage will induce cell cycle arrest. We examined the expression of *WEE1* and *SMR4, 5* and *7,* cell cycle regulators that are activated by DNA damage and replication stress (3,5). As shown in Figure 8A, the expression levels of *WEE1, SMR4* and *5* were not strongly altered in *sav6*, whereas the expression of *SMR7* was highly induced. Such induction was partially rescued by introduction of the *SAV6* gene (Supplementary Figure S6A). These results suggest that DNA damage in *sav6* mutants may affect the cell cycle through an SMR7-mediated pathway. To understand how the expression of *SMR7* may be activated, we examined the expression profile of *SMR7* in response to UV-C and various genotoxic chemicals. As shown in Supplementary Figure S6B and S6C, by hour 12 treatment, *SMR7* was strongly induced by Zeocin, CPT and UV-C, weakly and slowly induced by HU, and not induced by Aphidicolin. Therefore, the expression profile of *SMR7* indicates that it is highly responsive to UV-C and reagents that induce DSBs. Because UV-C treatment also produces single strand and double strand DNA breaks (41), the above results further imply that the DNA damage-associated phenotypes in the *sav6* mutant may be due to DSBs.

To evaluate how elevated expression of *SMR7* affects root development, we over-expressed *SMR7* in wild type seedlings. As shown in Figure 8B, over-expression of *SMR7* reduced the size of the RAM. However, the development of the QC cells was not affected. Therefore, elevated expression of *SMR7* in *sav6* may affect the development of the RAM, but not QC, which partially explains the phenotype of *sav6*.

It is widely believed that in response to DNA damage stress, the cell cycle is arrested to prevent damaged DNA from passing into the next generation. To evaluate whether upregulated expression of *SMR7* helps root cells to reduce DNA damage, we generated *35S:amiR172-SMR7/sav6* transgenic plants to knock down the expression of *SMR7* in *sav6* by over-expressing an *SMR7*-targeted microRNA. As shown in Supplementary Figure S6D, the expression of *SMR7* was strongly reduced in the transgenic lines compared to *sav6*. To evaluate DNA damage-induced cell death in *sav6* and *35S:amiR172-SMR7/sav6*, low concentrations of Zeocin (20 or 40 μg/ml) were used. As shown

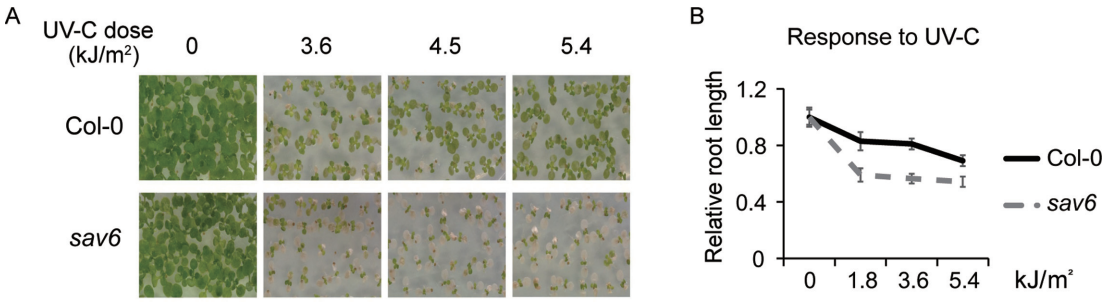

Figure 6. *sav6* is hypersensitive to UV-C. (**A**) Seedling responses of *sav6* to various doses of UV-C. (**B**) Root response of *sav6* to UV-C. Error bars represent the SEM ($n \geq 13$).

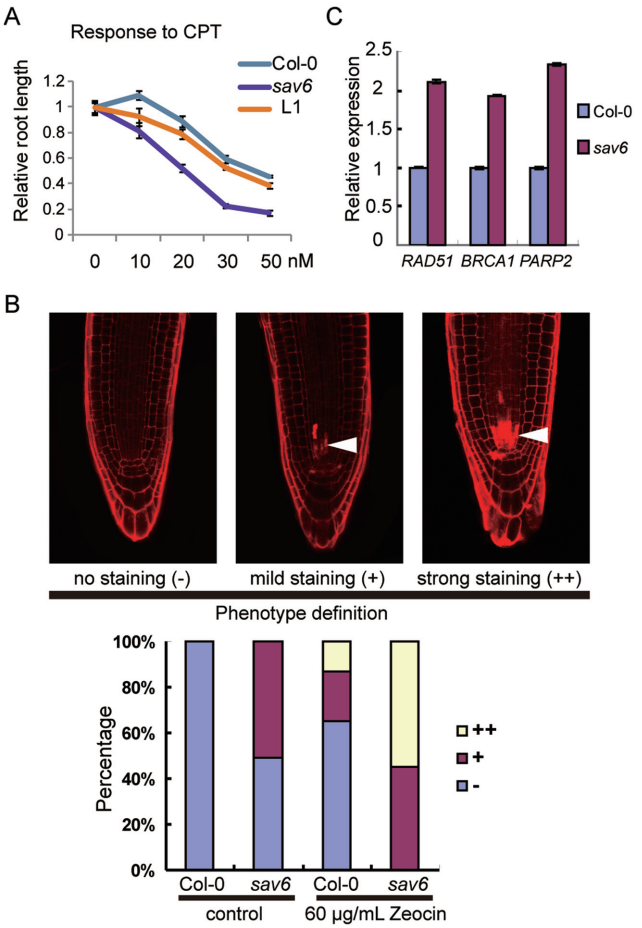

Figure 7. *sav6* exhibits enhanced responses to DNA damages. (**A**) The roots of *sav6* were hypersensitive to CPT-induced growth inhibition. L1 is one of the $SAV6_{pro}$*:SAV6/sav6* transgenic lines ($n \geq 12$). (**B**) *sav6* is hypersensitive to Zeocin. Dead cells were detected by propidium iodide (PI) staining. Upper panel: examples of no staining (-), mild staining (+) and strong staining (++); lower panel: percentage of cells in each category. Arrow heads indicate where cell death occurs ($n \geq 22$). (**C**) Quantitative reverse transcription PCR (qRT-PCR) results showing the relative expression of *RAD51*, *BRCA1* and *PARP2* in *sav6* versus that in Col-0 ($n = 3$). Error bars represent the SEM.

in Figure 8C, there are more dead cells in *35S:amiR172-SMR7/sav6* compared to *sav6*, as evidenced by a higher percentage of cells showing strong staining. This result indicates that elevated expression of *SMR7* in *sav6* helps to reduce DNA damage-induced cell death.

Constitutively activated DNA stress response pathways promote QC division through elevated *ERF115* and *PSK5* expression, which eventually leads to the loss of QC identity

QC cells rarely divide. It was therefore surprising to see that mutation of *SAV6* would disrupt QC development. Heyman *et al.* reported that bleomycin, a radiomimetic DSB-inducing drug, triggers programmed cell death of stem cells around the QC. They demonstrated that when these seedlings were transferred to a bleomycin-free medium later, the number of cells expressing QC marker gene, *WOX5,* increased, which may be associated with the activation of *PSK5* (6). We therefore examined the expression of *PSK5* in *sav6* seedlings and discovered that its expression was significantly elevated in *sav6* roots (Figure 9A). Furthermore, the expression of *PSKR1*, encoding a PSKα receptor, and *ERF115*, which is a rate-limiting transcription factor that directly activates *PSK5* expression, was also up-regulated in *sav6* (Figure 9A). The altered expression of all three genes was fully or partially rescued by introduction of the *SAV6* gene (Supplementary Figure S7). We therefore propose that the constitutively activated DNA stress response pathways in *sav6* may induce QC cell division through increased *PSK5* expression, which subsequently leads to the loss of QC identity in those cells.

To test this hypothesis, we first examined if constitutively elevated *PSK5* expression would affect QC development. Brassinosteroids induce the expression of *ERF115*, which subsequently activates *PSK5* expression (6) without inducing DNA lesions. Indeed, as shown in Supplementary Figure S8A, wild type seedlings grown on BL for 7 days exhibited elevated *PSK5* expression in roots, which was similar to the response to Zeocin treatment. We then examined the phenotypes of *QC46:GUS* and $WOX5_{pro}$*:GFP* seedlings grown on $\frac{1}{2}$ MS medium supplemented with various concentrations of BL for 7 days. As shown in Supplementary Figure S8B, the intensity of GUS staining in the root tips reduced as the BL concentrations increased, indicating the loss of QC cells. Similarly, expression of *WOX5* exhibited reduced intensity, and showed a more diffuse expression pattern as the concentrations of BL increased. WOX5 was reported to inhibit cell division (42). Reduced cellular expression of *WOX5* may therefore allow QC cell division to oc-

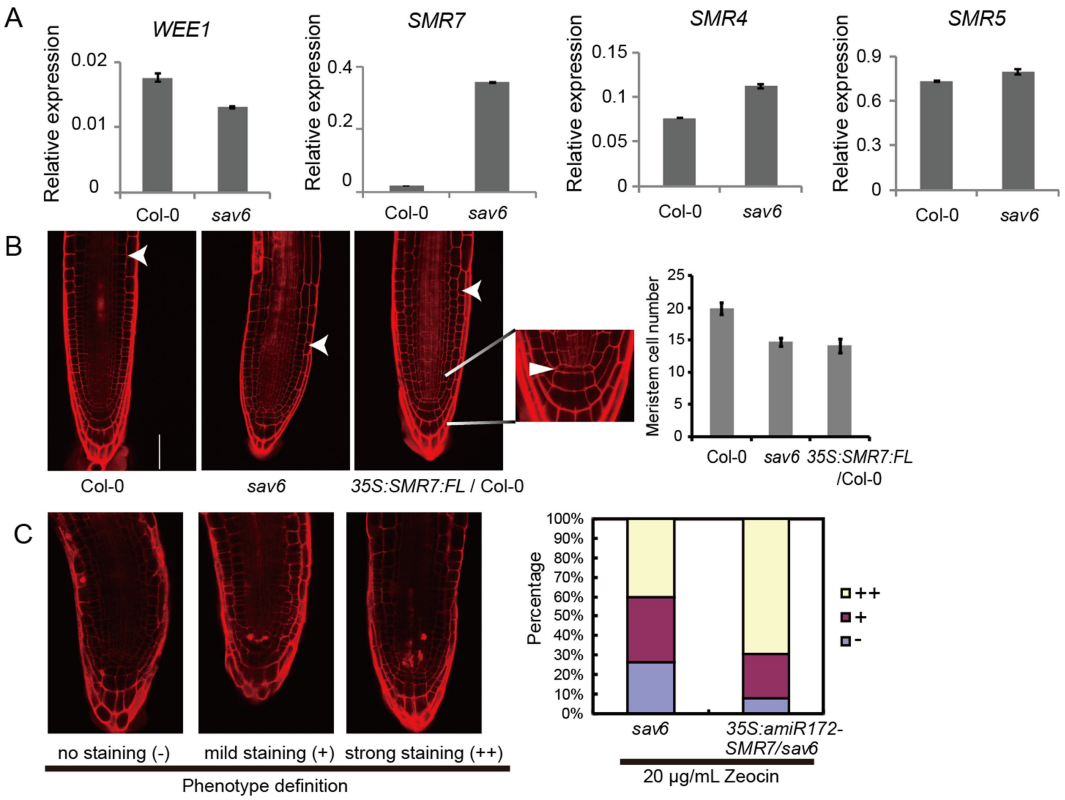

Figure 8. Elevated *SMR7* expression in *sav6* may affect RAM development. (**A**) qRT-PCR results showing the relative expression (normalized using the reference gene) of *WEE1, SMR4, 5* and *7* in Col-0 and *sav6* ($n = 3$). (**B**) *SMR7*-overexpression leads to reduced RAM size. Left panel: representative figures of PI-stained Col-0, *sav6* and *35S:SMR7:3XFLAG* root tips (arrowheads mark the RAM upper border); the arrowhead in the inset marks the QC cells; right panel: number of cortex cells in the RAM ($n \geq 11$); scale bars represent 50 μM. (**C**) Knocking down the expression of *SMR7* in *sav6* increases the susceptibility of the transgenic line (*35S:amiR172-SMR7/sav6*) to Zeocin. Dead cells were detected by PI staining. Left panel: examples of no staining (-), mild staining (+) and strong staining (++); right panel: percentage of cells in each category. The experiment was repeated three times in total and similar patterns were observed each time. Error bars represent the SEM.

cur. We hypothesize that the expanded *WOX5* expression domain, but reduced *WOX5* expression level, eventually results in the loss of QC.

We further tested how genotoxic reagents affect QC development. *QC46:GUS* and *WOX5$_{pro}$:GFP* seedlings were then grown on $\frac{1}{2}$ MS medium supplemented with various concentrations of Zeocin or CPT for 7 days. As shown in Figure 9B and Supplementary Figure S9, similar to the BL treatment, low concentrations of Zeocin and CPT also expanded the *WOX5*-expression domain. When the concentrations of these chemicals further increased, the expression of *WOX5* decreased significantly. The GUS signal of the QC46 marker genes did not show an increased expression domain, but became undetectable once the *WOX5* expression domain increased, suggesting that QC identity may be lost before the complete disappearance of the WOX5 signal. In summary, the above results suggested that prolonged exposure to genotoxic reagents may promote QC cell division through the activation of *PSK5*, which eventually leads to the loss of their QC identity. Similarly, defects in QC development in *sav6* may result from a constitutively active DNA stress response.

DISCUSSION

SAV6 encodes an AtFEN1 with FEN and GEN activity

In this study, we isolated an *Arabidopsis sav6* mutant that contains a point mutation in a putative At*FEN1* gene. BLAST results suggested that SAV6 may be the only FEN1 homologue in *Arabidopsis*, as its two closest homologues are *At1g01880* and *UVH3* (Figure 3A) and the latter was demonstrated to encode a RAD2/XPG gene product(33). *SAV6* complemented the temperature and UV-C hypersensitivity, but not the EMS hypersensitivity of the yeast *Δrad27 (fen1)* mutant, suggesting that the biochemical properties of SAV6 are different from those of Rad27 (Figure 3B). Comparing the nuclease activity profile of SAV6 and hFEN1, we found that SAV6 was only active on some of the FEN1 substrates. Compared to hFEN1, SAV6 possesses comparable double-flap endonuclease activity, weaker GEN activity towards bubble DNA structures and flap endonuclease activity towards substrates with a single-flap structure, but lacks the 5′ exonuclease activity towards DNA substrates with a nick on one strand, and GEN activity towards gapped DNA without any flap (Figure 4A–E). A double-flapped DNA structure with a 3′ single nucleotide flap was demonstrated to be the preferred substrate for the prokaryotic FEN1 homologue, the

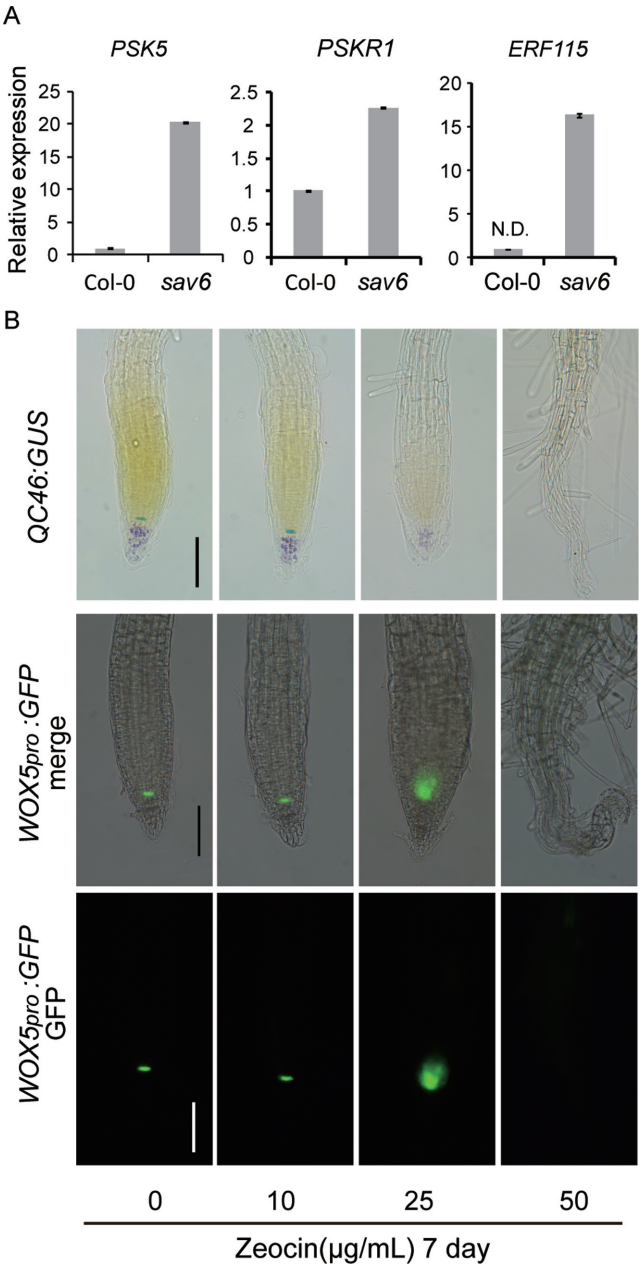

Figure 9. QC defects of *sav6* correlates with elevated *ERF115* and *PSK5* signalling. (**A**) qRT-PCR results showing the elevated expression of *PSK5, PSKR1* and *ERF115* in root tips of seedlings grow in Wc for 3 days. As the expression of *ERF115* was not detected in Col-0, the relative expression of *ERF115* to the reference gene is shown here. N.D.: not detected. Error bars represent the SEM ($n = 3$). (**B**) Long exposure to Zeocin abolished the expression of QC marker genes. *QC46:GUS* and $WOX5_{pro}$*:GFP* transgenic lines were sown and grown on $\frac{1}{2}$ MS medium supplemented with various concentrations of Zeocin for 7 days. GUS expression and GFP signals in root tips are shown. Scale bars represent 100 μM.

5′-nuclease domain associated with DNA polymerase I and yeast FEN1 (36,43). It was also suggested to be the preferred cellular substrate of FEN1 (36). Kao *et al.* proposed that when RNA primers in Okazaki fragments are removed during DNA replication, an equilibration between single-flap and double-flap structures occurs. FEN1 may only cleave double-flap structures containing a 1 nt 3′ tail (36). GEN activity on the bubble DNA substrates can be translated into the ability to repair stalled replication forks (44). Together with other 5′ exonucleases, the GEN activity of SAV6 may also enable it to resolve structured flaps during the maturation of Okazaki fragments. Therefore, despite the differences in the substrate preference between SAV6 and FEN1, SAV6 may still fulfil all the tasks of hFEN1 in DNA replication and repair of damaged DNAs. Consistent with its roles in DNA metabolism, YFP tagged SAV6 localizes to the nucleus. In addition, in some of the cells, SAV6 localizes to specific nuclear foci. Guo *et al.* discovered that FEN1 super-accumulates in the nucleolus in HeLa cells and plays a role in the maintenance of rDNA stability (38). To test this hypothesis, we examined the localization of SAV6 in the presence of DAPI stain (Supplementary Figure S3C). The nucleolus is not stained with DAPI, which appears as a dark circle inside of the blue nucleus. Most of the SAV6 speckles do not localize to the nucleolus, suggesting that these nuclear foci formed by SAV6 are not involved in the maintenance of rDNA stability. The patterns of these speckles look similar to those of the chromocenters. It would be interesting to see if the formation of these speckles is regulated or correlates with DNA repair. Furthermore, as the EXO or GEN activity of FEN1 can be greatly stimulated by its interacting proteins (27,45,46), it would be of interest to identify proteins that may interact with SAV6 and regulate its activity *in vivo*.

Developmental defects of *sav6*

Null mutations in *Rad27*, a yeast FEN1 homologue, result in slow growth, hypersensitivity to DNA damaging reagents and genome instability, whereas homozygous *Fen1* knockout in mice is embryonic lethal (11–13). When grown under normal conditions, the most obvious phenotypes of *sav6* are the short hypocotyls and primary roots, which were both completely rescued by genomic *SAV6*. In *sav6*, the mutation reduces the splicing efficiency of *SAV6*, and it is therefore a knock-down mutant of *SAV6*, which explains the rather mild phenotype of this mutant. Expression pattern analysis revealed that *SAV6* is highly expressed in tissues with rapidly dividing cells, such as root and shoot apical meristems, lateral root primordia, and progenitor cells of the stomatal lineage. It is also expressed in cells that undergo endoreplication, such as trichomes. Therefore, SAV6 may be required for DNA replication as well as DNA repair, a hypothesis that remains to be confirmed using a strong or null *sav6* mutant.

We observed that primary roots of *sav6* stopped growing a few days after germination. A lateral root emerged to replace the primary root (Supplementary Figure S1A). The cellular organization of RAM in this lateral root is also abnormal (Supplementary Figure S1D). As this lateral root can grow much longer compared to the primary root (Supplementary Figure S1B), its defect in RAM may not be as severe as that observed in the primary root. We speculate that the severity of the defect may be associated with the cell division rates. Alternatively, at different developmental stages, different degrees of DNA stresses may be encountered, which affects the severity of the phenotype. After be-

ing transferred to soil, *sav6* mutants grow normally (Supplementary Figure S10A), indicating that there are other mechanisms to compensate for the developmental defects associated with *sav6*.

Phenotypes of the *sav6* mutant suggest that *AtFEN1* is required for DNA damage repair and maintenance of genome integrity

FEN1 is best known for its role in Okazaki fragment maturation and long-patch BER and is believed to play an important role in DNA replication and responses to DNA damage (11). We found that *sav6* responded normally to HU (Supplementary Figure S5A), whereas it was hypersensitive to chemicals that induce DSBs (CPT and Zeocin, Figure 7A and B). UV-C treatment is also capable of inducing single- and double-stranded DNA breaks and *sav6* is hypersensitive to UV-C as well. In addition, the expression levels of several DNA damage-activated genes and one DSB-specific induced gene were elevated in *sav6* (Figure 7C and Supplementary Figure S5D), suggesting that it is required for the maintenance of DNA integrity. Furthermore, the expression of *SMR7* is also highly induced in *sav6* (Figure 8A). The expression of *SMR7* is strongly induced by DSB-inducing reagents, but not by Aphidicolin, which blocks DNA replication. Finally, seedlings treated with DSB-inducing reagents, but not Aphidicolin, exhibited cell death in meristem cells and their early descendents (7) and we also observed cell death in *sav6* roots without any treatment. Together, the above data indicate that SAV6 is required for both the maintenance of genome integrity and response to DNA damage. Reduced expression of *SAV6* may lead to DSBs, but has limited impact on DNA replication. Consistent with the above hypothesis, we found no obvious defect in endoreplication-regulated processes, such as trichome development (Supplementary Figure S10B). Surprisingly, we found that the genomic SAV6 only partially suppressed the Zeocin/CPT hypersensitivity and the enhanced expression of *SMR7* and DNA damage response genes in *sav6* mutants (Supplementary Figure S5B, S5C and S6A). We speculate that the original *sav6* mutant may contain other mutations that affect the response to DNA damage, as the $SAV6_{pro}$*:SAV6g*/*sav6* transgenic plants were generated using the original *sav6* mutant but not the one backcrossed to Col-0 for three generations. Alternatively, the presence of enhancers outside of the transgene we used could explain the partial rescue phenotype. Because the described phenotypes were partially suppressed by introduction of a genomic *SAV6* transgene and the characterization of the *sav6* mutant was performed using the *sav6* mutant that was backcrossed to Col-0 for three generations, we believe our conclusions should still be reliable.

Recently, Saharia *et al.* demonstrated that FEN1 depletion did not affect cell cycle progression or *in vitro* DNA replication through non-telomeric sequences. Instead, it may maintain telomere stability by facilitating replication through the G-rich lagging strand and ensuring high fidelity telomere replication (47). Telomeres protect chromosome ends from being recognized as DSBs and help to solve the end replication problem associated with linear genomic DNA. Consistent with this report, we found that SAV6 knockdown induced DSB-activated stress responses, but generated minimal DNA replication stress. This phenotype is reminiscent of the *Arabidopsis MERISTEM DISORGANIZATION 1 (mdo1–1)* mutant, which exhibits phenotypes very similar to *sav6*, including retarded root growth, defects in RAM development and maintenance of QC cells, cell death at root tips and activation of *RAD51* and *BRCA1* (48). *MDO1* encodes the AtTEN1, which is part of the trimeric replication protein A (RPA)-like CST (Cdc13/Stn1/ Ten1) complex and is required for the functions of telomeres. We therefore speculate that the root defects of *sav6* may result from defects in telomere maintenance, which may generate DSB stress and subsequently affect RAM development.

sav6 is hypersensitive to UV-C

In animal cells, it is proposed that FEN1 may introduce DSBs when the DNA replication forks are stalled by UV cross-links and therefore induce recombination repair (27,38). In support of this hypothesis, it is required for recovery from UV-C induced replication inhibition (11,49). Using the yeast system, it was demonstrated that the FEN activity of FEN1 is not required for this recovery process (27). We have shown that SAV6 is also required for the recovery from UV-C stress using both the yeast and *Arabidopsis* systems (Figures 3B and 6). Because SAV6 lacks EXO activity, our data therefore hint that the GEN activity may be critical for the recovery from UV-C induced DNA damage.

Elevated *SMR7* in *sav6* inhibits growth of RAM, but does not affect QC development

Yi *et al.* reported that transcription of *SMR4, 5* and *7* were strongly induced by reactive oxygen species in an ATM-dependent manner (5). They demonstrated that these cyclin-dependent kinase inhibitors possess cell cycle inhibitory potential. We discovered that in *sav6*, only the expression of *SMR7* was strongly induced, whereas *SMR4* and *SMR5* were slightly induced or not induced at all (Figure 8A). Transgenic seedlings constitutively expressing high levels of *SMR7* exhibited short RAMs, suggesting that the division of RAM cells may be inhibited. Interestingly, QC cells are clearly visible in SMR7 over-expressing seedlings, therefore the maintenance of the QC is not affected by SMR7 over-expression and the QC defect of *sav6* may be mediated by other factors.

Constitutively elevated *PSK5* expression in *sav6* affects QC development

PSK5 promotes QC division. Heyman *et al.* showed that after 24 h of bleomycin treatment, the *WOX5*-expressing domain increased during the recovery process. In the *sav6* mutant, *PSK5* expression increased, but the root domains expressing the QC markers (*WOX5, QC46*, *QC25*, Figure 5E and Supplementary Figure S4) were reduced, which seems to be inconsistent with the previous observations. We hypothesize that long-term exposure to DSB stress may activate QC cell division in order to replenish dead stem cells.

Because these cells are not quiescent anymore, they become actively dividing and eventually may lose QC identity. In fact, we observed an increase in the *WOX5* expression domain size after low levels of DSB stress, which is accompanied by a decrease in intensity. The increased *WOX5* expression domain may result from QC division, while the decreased *WOX5* signal may suggest that WOX5-mediated signalling is altered. These results support the hypothesis that QC cell division is activated by DSB stress, which precedes the loss of QC identity, and results in a complete disappearance of *WOX5* signal. Furthermore, because brassinosteroid treatment elevated the expression of *ERF115* and *PSK5* and resulted in the loss of QC, it is likely that prolonged activation of *ERF115/PSK5* signalling alone may be sufficient to cause the loss of QC. In *sav6* mutants, the loss of QC cells may partially contribute to the reduced RAM size and short root phenotype, along with the activation of SMR7-mediated cell cycle regulation.

ACCESSION NUMBER

Sequence data from this article can be found in the Arabidopsis Genome Initiative or National Center for Biotechnology Information (NCBI) databases under the following accession numbers: *REF3* (*At1g13320*), *SAV6* (*At5g26680*), *SMR7* (*At3g27630*), *PSK5* (*At5g65870*), *ATPSKR1* (*At2g02220*), *RAD51* (*At5g20850*), *BRCA1* (*At4g21070*), *PARP2* (*At4g02390*), *RAD27* (*NP012809.1*), *HsaFEN1* (*NP004102.1*), *DreFEN1* (*NP942115.1*), *Dme FEN1* (*NP523765.1*), *MmuFEN1* (*NP0320252.2*), *OsFEN1a* (*AB021666*), *OsFEN1b* (*AB088391*), *UVH3* (*At3g28030*), *SMR4* (*At5g02220*), *SMR5* (*At1g07500*), *WEE1* (*At1g02970*) and *ERF115* (*At5g07310*).

SUPPLEMENTARY DATA

Supplementary Data are available at NAR Online.

ACKNOWLEDGEMENTS

We thank Dr Nancy Linford for critical reading; Dr Michael S. Reagan for providing the yeast SX46A and Δ*rad27:TRP1* mutant strain; Dr Huang, Tao for providing *QC46*:*GUS*, *QC25*:*GUS* seeds and the *pDONR201-miR172a* vector; and Dr S. Savaldi-Goldstein for *WOX5* $_{pro}$:*GFP* seeds.

FUNDING

National Natural Science Foundation of China [31171162, 31271298 to Y.T]; Fundamental Research Funds for the Central Universities of China [2010121090, 2012121041 to Y.T.]; 111 Project [B12001 to Y.T.]; National Institutes of Health [RO1CA076734 to B.H.S.]. Early studies for this manuscript were performed in the Chory laboratory at The Salk Institute for Biological Studies and were supported by the Howard Hughes Medical Institute and the US National Institutes of Health [R01GM52413 to Joanne Chory]. Funding for open access charge: National Natural Science Foundation of China[31171162,31271298 to Y.T].
Conflict of interest statement. None declared.

REFERENCES

1. Scheres,B., Benfey,P. and Dolan,L. (2002) Root development. *Arabidopsis Book*, **1**, e0101.
2. van den Berg,C., Willemsen,V., Hendriks,G., Weisbeek,P. and Scheres,B. (1997) Short-range control of cell differentiation in the Arabidopsis root meristem. *Nature*, **390**, 287–289.
3. De Schutter,K., Joubes,J., Cools,T., Verkest,A., Corellou,F., Babiychuk,E., Van Der Schueren,E., Beeckman,T., Kushnir,S., Inze,D. *et al.* (2007) Arabidopsis WEE1 kinase controls cell cycle arrest in response to activation of the DNA integrity checkpoint. *Plant Cell*, **19**, 211–225.
4. Cools,T., Iantcheva,A., Weimer,A.K., Boens,S., Takahashi,N., Maes,S., Van den Daele,H., Van Isterdael,G., Schnittger,A. and De Veylder,L. (2011) The Arabidopsis thaliana checkpoint kinase WEE1 protects against premature vascular differentiation during replication stress. *Plant Cell*, **23**, 1435–1448.
5. Yi,D., Alvim Kamei,C.L., Cools,T., Vanderauwera,S., Takahashi,N., Okushima,Y., Eekhout,T., Yoshiyama,K.O., Larkin,J., Van den Daele,H. *et al.* (2014) The Arabidopsis SIAMESE-RELATED cyclin-dependent kinase inhibitors SMR5 and SMR7 regulate the DNA damage checkpoint in response to reactive oxygen species. *Plant Cell*, **26**, 296–309.
6. Heyman,J., Cools,T., Vandenbussche,F., Heyndrickx,K.S., Van Leene,J., Vercauteren,I., Vanderauwera,S., Vandepoele,K., De Jaeger,G., Van Der Straeten,D. *et al.* (2013) ERF115 controls root quiescent center cell division and stem cell replenishment. *Science*, **342**, 860–863.
7. Fulcher,N. and Sablowski,R. (2009) Hypersensitivity to DNA damage in plant stem cell niches. *Proc. Natl. Acad. Sci. U.S.A.*, **106**, 20984–20988.
8. Marciniak,K. and Bilecka,A. (1985) Changes in nuclear, nucleolar and cytoplasmic RNA content during growth and differentiation of root parenchyma cells in plant species with different dynamics of DNA endoreplication. *Folia Histochem. Cytobiol.*, **23**, 231–245.
9. Singh,P., Zheng,L., Chavez,V., Qiu,J. and Shen,B. (2007) Concerted action of exonuclease and Gap-dependent endonuclease activities of FEN-1 contributes to the resolution of triplet repeat sequences (CTG)n- and (GAA)n-derived secondary structures formed during maturation of Okazaki fragments. *J. Biol. Chem.*, **282**, 3465–3477.
10. Zheng,L., Jia,J., Finger,L.D., Guo,Z., Zer,C. and Shen,B. (2011) Functional regulation of FEN1 nuclease and its link to cancer. *Nucleic Acids Res.*, **39**, 781–794.
11. Reagan,M.S., Pittenger,C., Siede,W. and Friedberg,E.C. (1995) Characterization of a mutant strain of Saccharomyces cerevisiae with a deletion of the RAD27 gene, a structural homolog of the RAD2 nucleotide excision repair gene. *J. Bacteriol.*, **177**, 364–371.
12. Johnson,R.E., Kovvali,G.K., Prakash,L. and Prakash,S. (1995) Requirement of the yeast RTH1 5′ to 3′ exonuclease for the stability of simple repetitive DNA. *Science*, **269**, 238–240.
13. Larsen,E., Gran,C., Saether,B.E., Seeberg,E. and Klungland,A. (2003) Proliferation failure and gamma radiation sensitivity of Fen1 null mutant mice at the blastocyst stage. *Mol. Cell. Biol.*, **23**, 5346–5353.
14. Kimura,S., Furukawa,T., Kasai,N., Mori,Y., Kitamoto,H.K., Sugawara,F., Hashimoto,J. and Sakaguchi,K. (2003) Functional characterization of two flap endonuclease-1 homologues in rice. *Gene*, **314**, 63–71.
15. Kimura,S., Ueda,T., Hatanaka,M., Takenouchi,M., Hashimoto,J. and Sakaguchi,K. (2000) Plant homologue of flap endonuclease-1: molecular cloning, characterization, and evidence of expression in meristematic tissues. *Plant Mol. Biol.*, **42**, 415–427.
16. Sabatini,S., Heidstra,R., Wildwater,M. and Scheres,B. (2003) SCARECROW is involved in positioning the stem cell niche in the Arabidopsis root meristem. *Genes Dev.*, **17**, 354–358.
17. Nawy,T., Lee,J.Y., Colinas,J., Wang,J.Y., Thongrod,S.C., Malamy,J.E., Birnbaum,K. and Benfey,P.N. (2005) Transcriptional profile of the Arabidopsis root quiescent center. *Plant Cell*, **17**, 1908–1925.
18. Czechowski,T., Stitt,M., Altmann,T., Udvardi,M.K. and Scheible,W.R. (2005) Genome-wide identification and testing of superior reference genes for transcript normalization in Arabidopsis. *Plant Physiol.*, **139**, 5–17.

19. Jefferson,R.A., Kavanagh,T.A. and Bevan,M.W. (1987) GUS fusions: beta-glucuronidase as a sensitive and versatile gene fusion marker in higher plants. *EMBO J.*, **6**, 3901–3907.
20. Wysocka-Diller,J.W., Helariutta,Y., Fukaki,H., Malamy,J. and Benfey,P. (2000) Molecular analysis of SCARECROW function reveals a radial patterning mechanism common to root and shoot. *Development*, **127**, 595–603.
21. Zhang,W., To,J.P., Cheng,C.Y., Schaller,G.E. and Kieber,J.J. (2011) Type-A response regulators are required for proper root apical meristem function through post-transcriptional regulation of PIN auxin efflux carriers. *Plant J.*, **68**, 1–10.
22. Tao,Y., Ferrer,J.L., Ljung,K., Pojer,F., Hong,F., Long,J.A., Li,L., Moreno,J.E., Bowman,M.E., Ivans,L.J. *et al.* (2008) Rapid synthesis of auxin via a new tryptophan-dependent pathway is required for shade avoidance in plants. *Cell*, **133**, 164–176.
23. Wang,X., Li,X., Meisenhelder,J., Hunter,T., Yoshida,S., Asami,T. and Chory,J. (2005) Autoregulation and homodimerization are involved in the activation of the plant steroid receptor BRI1. *Dev. Cell*, **8**, 855–865.
24. Schwab,R., Ossowski,S., Riester,M., Warthmann,N. and Weigel,D. (2006) Highly specific gene silencing by artificial microRNAs in Arabidopsis. *Plant Cell*, **18**, 1121–1133.
25. Frank,G., Qiu,J., Zheng,L. and Shen,B. (2001) Stimulation of eukaryotic flap endonuclease-1 activities by proliferating cell nuclear antigen (PCNA) is independent of its in vitro interaction via a consensus PCNA binding region. *J. Biol. Chem.*, **276**, 36295–36302.
26. Guo,Z., Chavez,V., Singh,P., Finger,L.D., Hang,H., Hegde,M.L. and Shen,B. (2008) Comprehensive mapping of the C-terminus of flap endonuclease-1 reveals distinct interaction sites for five proteins that represent different DNA replication and repair pathways. *J. Mol. Biol.*, **377**, 679–690.
27. Zheng,L., Zhou,M., Chai,Q., Parrish,J., Xue,D., Patrick,S.M., Turchi,J.J., Yannone,S.M., Chen,D. and Shen,B. (2005) Novel function of the flap endonuclease 1 complex in processing stalled DNA replication forks. *EMBO Rep.*, **6**, 83–89.
28. Zheng,L., Dai,H., Zhou,M., Li,M., Singh,P., Qiu,J., Tsark,W., Huang,Q., Kernstine,K., Zhang,X. *et al.* (2007) Fen1 mutations result in autoimmunity, chronic inflammation and cancers. *Nat. Med.*, **13**, 812–819.
29. Lukowitz,W., Gillmor,C.S. and Scheible,W.R. (2000) Positional cloning in Arabidopsis. Why it feels good to have a genome initiative working for you. *Plant Physiol.*, **123**, 795–805.
30. Traas,J., Hulskamp,M., Gendreau,E. and Hofte,H. (1998) Endoreduplication and development: rule without dividing? *Curr. Opin. Plant Biol.*, **1**, 498–503.
31. Churchman,M.L., Brown,M.L., Kato,N., Kirik,V., Hulskamp,M., Inze,D., De Veylder,L., Walker,J.D., Zheng,Z., Oppenheimer,D.G. *et al.* (2006) SIAMESE, a plant-specific cell cycle regulator, controls endoreplication onset in Arabidopsis thaliana. *Plant Cell*, **18**, 3145–3157.
32. Oppenheimer,D.G. (1998) Genetics of plant cell shape. *Curr. Opin. Plant Biol.*, **1**, 520–524.
33. Liu,Z., Hall,J.D. and Mount,D.W. (2001) Arabidopsis UVH3 gene is a homolog of the Saccharomyces cerevisiae RAD2 and human XPG DNA repair genes. *Plant J.*, **26**, 329–338.
34. Qiu,J., Li,X., Frank,G. and Shen,B. (2001) Cell cycle-dependent and DNA damage-inducible nuclear localization of FEN-1 nuclease is consistent with its dual functions in DNA replication and repair. *J. Biol. Chem.*, **276**, 4901–4908.
35. Hansen,R.J., Friedberg,E.C. and Reagan,M.S. (2000) Sensitivity of a S. cerevisiae RAD27 deletion mutant to DNA-damaging agents and in vivo complementation by the human FEN-1 gene. *Mutat. Res.*, **461**, 243–248.
36. Kao,H.I., Henricksen,L.A., Liu,Y. and Bambara,R.A. (2002) Cleavage specificity of Saccharomyces cerevisiae flap endonuclease 1 suggests a double-flap structure as the cellular substrate. *J. Biol. Chem.*, **277**, 14379–14389.
37. Vandenbussche,F., Verbelen,J.P. and Van Der Straeten,D. (2005) Of light and length: regulation of hypocotyl growth in Arabidopsis. *Bioessays*, **27**, 275–284.
38. Guo,Z., Qian,L., Liu,R., Dai,H., Zhou,M., Zheng,L. and Shen,B. (2008) Nucleolar localization and dynamic roles of flap endonuclease 1 in ribosomal DNA replication and damage repair. *Mol. Cell. Biol.*, **28**, 4310–4319.
39. Doucet-Chabeaud,G., Godon,C., Brutesco,C., de Murcia,G. and Kazmaier,M. (2001) Ionising radiation induces the expression of PARP-1 and PARP-2 genes in Arabidopsis. *Mol. Genet. Genomics*, **265**, 954–963.
40. Chen,I.P., Haehnel,U., Altschmied,L., Schubert,I. and Puchta,H. (2003) The transcriptional response of Arabidopsis to genotoxic stress - a high-density colony array study (HDCA). *Plant J.*, **35**, 771–786.
41. Foresti,M. and Avallone,B. (2008) Only complete rejoining of DNA strand breaks after UVC allows K562 cell proliferation and DMSO induction of erythropoiesis. *J. Photochem. Photobiol. B*, **90**, 8–16.
42. Forzani,C., Aichinger,E., Sornay,E., Willemsen,V., Laux,T., Dewitte,W. and Murray,J.A. (2014) WOX5 suppresses CYCLIN D activity to establish quiescence at the center of the root stem cell niche. *Curr. Biol.*, **24**, 1939–1944.
43. Xu,Y., Potapova,O., Leschziner,A.E., Grindley,N.D. and Joyce,C.M. (2001) Contacts between the 5′ nuclease of DNA polymerase I and its DNA substrate. *J. Biol. Chem.*, **276**, 30167–30177.
44. Chung,L., Onyango,D., Guo,Z., Jia,P., Dai,H., Liu,S., Zhou,M., Lin,W., Pang,I., Li,H. *et al.* (2015) The FEN1 E359K germline mutation disrupts the FEN1-WRN interaction and FEN1 GEN activity, causing aneuploidy-associated cancers. *Oncogene*, **34**, 902–911.
45. Tom,S., Henricksen,L.A. and Bambara,R.A. (2000) Mechanism whereby proliferating cell nuclear antigen stimulates flap endonuclease 1. *J. Biol. Chem.*, **275**, 10498–10505.
46. Parrish,J.Z., Yang,C., Shen,B. and Xue,D. (2003) CRN-1,a Caenorhabditis elegans FEN-1 homologue, cooperates with CPS-6/EndoG to promote apoptotic DNA degradation. *EMBO J.*, **22**, 3451–3460.
47. Saharia,A., Teasley,D.C., Duxin,J.P., Dao,B., Chiappinelli,K.B. and Stewart,S.A. (2010) FEN1 ensures telomere stability by facilitating replication fork re-initiation. *J. Biol. Chem.*, **285**, 27057–27066.
48. Hashimura,Y. and Ueguchi,C. (2011) The Arabidopsis MERISTEM DISORGANIZATION 1 gene is required for the maintenance of stem cells through the reduction of DNA damage. *Plant J.*, **68**, 657–669.
49. Christmann,M., Tomicic,M.T., Origer,J. and Kaina,B. (2005) Fen1 is induced p53 dependently and involved in the recovery from UV-light-induced replication inhibition. *Oncogene*, **24**, 8304–8313.